

# Transient Ischemic Dilation Ratio in $^{82}\text{Rb}$ PET Myocardial Perfusion Imaging: Normal Values and Significance as a Diagnostic and Prognostic Marker

Christoph Rischpler<sup>1</sup>, Takahiro Higuchi<sup>1</sup>, Kenji Fukushima<sup>1</sup>, Mehrbod S. Javadi<sup>1</sup>, Jennifer Merrill<sup>1</sup>, Stephan G. Nekolla<sup>2</sup>, Paco E. Bravo<sup>1</sup>, and Frank M. Bengel<sup>1,3</sup>

<sup>1</sup>Division of Nuclear Medicine, Russell H. Morgan Department of Radiology, Johns Hopkins University, Baltimore, Maryland; <sup>2</sup>Nuklearmedizinische Klinik der Technischen Universität München, Munich, Germany; and <sup>3</sup>Department of Nuclear Medicine, Hannover Medical School, Hannover, Germany

In myocardial perfusion SPECT, transient ischemic dilation ratio (TID) is a well-established marker of severe ischemia and adverse outcome. However, its role in the setting of  $^{82}\text{Rb}$  PET is less well defined. **Methods:** We analyzed 265 subjects who underwent clinical rest–dipyridamole  $^{82}\text{Rb}$  PET/CT. Sixty-two subjects without a prior history of cardiac disease and with a normal myocardial perfusion study had either a low or a very low pretest likelihood of coronary artery disease or negative CT angiography. These subjects were used to establish a reference range of TID. In the remaining 203 patients with an intermediate or high pretest likelihood, subgroups with normal and abnormal TID were established and compared with respect to clinical variables, perfusion defect scores, left ventricular function, and absolute myocardial flow reserve. Follow-up was obtained for  $969 \pm 328$  d to determine mortality by review of the social security death index. **Results:** In the reference group, TID ratio was  $0.98 \pm 0.06$ . Accordingly, a threshold for abnormal TID was set at greater than 1.13 ( $0.98 + 2.5$  SDs). In the study group, 19 of 203 patients (9%) had an elevated TID ratio. Significant differences between subgroups with normal and abnormal TID ratio were observed for ejection fraction reserve ( $5.0 \pm 6.4$  vs.  $1.8 \pm 7.9$ ;  $P < 0.05$ ), difference between end-systolic volume (ESV) at rest and stress ( $\Delta\text{ESV}[\text{stress-rest}]$ ;  $1.8 \pm 7.4$  vs.  $12.3 \pm 13.0$  mL;  $P < 0.0001$ ), difference between end-diastolic volume (EDV) at rest and stress ( $\Delta\text{EDV}[\text{stress-rest}]$ ;  $10.8 \pm 11.5$  vs.  $23.8 \pm 14.6$  mL;  $P < 0.0001$ ), summed rest score ( $1.8 \pm 3.8$  vs.  $3.8 \pm 7.6$ ;  $P < 0.05$ ), summed stress score ( $3.0 \pm 5.4$  vs.  $7.5 \pm 9.8$ ;  $P < 0.002$ ), summed difference score ( $1.3 \pm 2.6$  vs.  $3.7 \pm 5.3$ ;  $P < 0.02$ ), and global myocardial flow reserve ( $2.1 \pm 0.8$  vs.  $1.7 \pm 0.6$ ;  $P < 0.02$ ). Additionally, TID-positive patients had a significantly lower overall survival probability ( $P < 0.05$ ). In a subgroup analysis of patients without regional perfusion abnormalities, TID-positive patients' overall survival probability was significantly smaller ( $P < 0.03$ ), and TID was an independent predictor (exponentiation of the B coefficients [ $\text{Exp}(b)$ ] = 6.22;  $P < 0.009$ ) together with an ejection fraction below 45% ( $\text{Exp}(b)$  = 6.16;  $P < 0.002$ ). **Conclusion:** The present study suggests a reference

range of TID for  $^{82}\text{Rb}$  PET myocardial perfusion imaging that is in the range of previously established values for SPECT. Abnormal TID in  $^{82}\text{Rb}$  PET is associated with more extensive left ventricular dysfunction, ischemic compromise, and reduced global flow reserve. Preliminary outcome analysis suggests that TID-positive subjects have a lower overall survival probability.

**Key Words:** positron emission tomography; myocardial perfusion imaging;  $^{82}\text{Rb}$ ; transient ischemic dilation

**J Nucl Med 2012; 53:723–730**

DOI: 10.2967/jnumed.111.097600

**P**ET using  $^{82}\text{Rb}$  is becoming a more widespread and attractive alternative to SPECT for myocardial perfusion imaging (1,2), not only because of the persistent shortage of  $^{99\text{m}}\text{Tc}$  (3) but also because of its superior diagnostic value for coronary artery disease (CAD) when compared with myocardial perfusion SPECT (2,4,5), its low radiation dose (6), its short acquisition time allowing multiple studies in 1 d (1,2), and its potential to quantify absolute myocardial blood flow (7). Nevertheless, some generally accepted parameters in myocardial perfusion SPECT have only been marginally investigated in  $^{82}\text{Rb}$  PET. The transient ischemic dilation ratio (TID), determined by the ratio of the stress endocardial volume and the rest endocardial volume in static nongated images, is a well-established marker of severe ischemia (8–10) and adverse outcome in myocardial perfusion SPECT (10,11), but its role in the setting of  $^{82}\text{Rb}$  PET is less well defined and needs to be further elucidated. The objective of this study was to determine the reference range of TID in  $^{82}\text{Rb}$  myocardial perfusion imaging and to investigate its relevance with respect to clinical variables, perfusion defect scores, left ventricular (LV) function, absolute coronary flow, and adverse outcome.

## MATERIALS AND METHODS

### Patients and Study Design

We retrospectively analyzed 265 consecutive patients who underwent clinical rest–dipyridamole  $^{82}\text{Rb}$  PET/CT myocardial

Received Aug. 28, 2011; revision accepted Dec. 27, 2011.

For correspondence or reprints contact: Frank M. Bengel, Department of Nuclear Medicine, Hannover Medical School, Carl-Neuberg-Strasse 1, D-30625 Hannover, Germany.

E-mail: [bengel.frank@mh-hannover.de](mailto:bengel.frank@mh-hannover.de)

Published online Apr. 9, 2012.

COPYRIGHT © 2012 by the Society of Nuclear Medicine, Inc.

perfusion scanning at Johns Hopkins Hospital. Only PET/CT studies with availability of all necessary image sets were included. A single PET/CT scan was obtained per patient.

A reference group for definition of the reference range of TID consisted of 62 subjects with no prior history of cardiac disease and without perfusion defects. Subjects were included in this group either because they had a low or very low pretest likelihood of CAD ( $\leq 10\%$ ) based on criteria by Diamond and Forrester (12) ( $n = 34$ ) or because they had negative CT angiography (CTA) results during the PET/CT session, showing complete absence of coronary atherosclerosis ( $n = 28$ ). General characteristics at the time of PET are summarized in Table 1. This group was already used for definition of reference ranges of LV functional measurements from gated PET in a prior publication, in which TID had not been analyzed (13).

In the remaining 203 patients, the study group, the mean age ( $\pm$ SD) was  $60 \pm 12$  y. The group consisted of 90 men and 113 women, with a mean body mass index of  $31.9 \pm 8.9$ . Regarding further risk factors, there were 71 subjects with a history of smoking, 134 patients with hypertension, 100 patients with hyperlipidemia, and 75 subjects with diabetes mellitus. Seventy-four patients had a history of CAD, 29 patients had prior myocardial infarction (MI), and 7 patients had been diagnosed with heart failure. Forty subjects received  $\beta$ -blockers, 44 were treated with either angiotensin-converting enzyme inhibitors or angiotensin receptor blockers, and 43 patients took statins at the time of the PET scan. In 136 patients, the scan was requested because of the patient's presentation with acute chest pain or shortness of breath. Twenty-eight patients were scanned for follow-up purposes—for example, because of a positive history of heart failure, MI, percutaneous coronary intervention, or coronary bypass grafts. Only 17 patients were referred for preoperative evaluation. Other indications were screening for CAD because of multiple risk factors ( $n = 7$ ), equivocal SPECT ( $n = 3$ ), syncope ( $n = 1$ ), or suspected cardiac sarcoidosis or cardiomyopathy ( $n = 7$ ). Two scans were obtained because of unknown reasons for hypertensive urgency or implanted cardioverter defibrillator triggering. In 4 patients, the scan was requested for more than one of these reasons: 3 patients were referred because of chest pain and a history of syncope and 1 patient was scanned because of shortness of breath and for follow-up. Taking these characteristics into account, this study group can be described as a heterogeneous assortment of patients with known CAD or an intermediate or high likelihood for CAD. A

detailed summary of the clinical characteristics can be found in Table 2.

Because of its retrospective nature, this study was granted exempt status by the Johns Hopkins Institutional Review Board.

### Acquisition Protocol

All images were acquired using a Discovery STRx PET/CT system (GE Healthcare). The PET component is equipped with a high-performance lutetium yttrium orthosilicate crystal scintillator, and the CT component consists of a 64-slice CT scanner. Patients were instructed to refrain from any caffeinated substances for 24 h and to fast for more than 4 h before testing. For attenuation correction, a low-dose CT scan (120 kV, 50–100 mA) was obtained before the rest–stress myocardial perfusion protocol was started.

For the rest acquisition, 1,480–1,850 MBq (40–50 mCi) of  $^{82}\text{Rb}$ -chloride were injected intravenously using the CardioGen-82  $^{82}\text{Sr}/^{82}\text{Rb}$  generator (Bracco Diagnostics Inc.). After the slow administration of  $^{82}\text{Rb}$  over 30 s, a 2-dimensional list-mode PET scan was obtained over a period of 8 min.

For the stress acquisition, dipyridamole (0.56 mg/kg) was applied for 4 min. Four additional minutes after vasodilation, a second dose of 1,480–1,850 MBq (40–50 mCi) of  $^{82}\text{Rb}$ -chloride was injected, and data were acquired as previously described for the rest scan. Subsequently, rest and stress PET data were aligned accurately with the CT scan, and attenuation correction was performed (14). Ultimately, resampling of the list-mode data to static (90-s prescan delay), gated (8 bins per cardiac cycle), and dynamic images (32 frames for 8 min:  $20 \times 6$  s,  $5 \times 12$  s,  $4 \times 30$  s, and  $3 \times 60$  s) was accomplished (15).

### Data Analysis

Acquired PET images were reconstructed with an iterative algorithm (ordered-subset expectation maximization, 2 iterations, 21 subsets) and postprocessing filtering (Butterworth, order of 10; cutoff, 0.25 cycles/bin). The acquired images were analyzed using the previously validated commercially available software CardIQ Physio (GE Healthcare) (16). Initially, the long axis was defined by oblique reorientation of the datasets on the transversal planes. Subsequently, the valve plane for gated and ungated images was specified, and quality control of automated contour detection was achieved. Ejection fraction (EF), end-systolic volume (ESV), end-diastolic volume (EDV), and stroke volume were automatically derived from rest and stress gated datasets, and TID was automatically obtained from nongated images. Examples of contouring and derived TIDs are shown in Figure 1.

*Assessment of Perfusion Defect Scores.* The perfusion defect scores—summed rest score (SRS) and summed stress score (SSS)—were derived as follows: the 17-segment model according to the American Heart Association was applied for each rest and stress study to the short- and long-axis myocardial tomograms, and scores were obtained using semiquantitative visual interpretation by an experienced reader (17). Briefly, to each segment a value between 0 (normal tracer uptake) and 4 (absence of tracer uptake) was assigned and added to obtain SSS and SRS, and finally the summed difference score (SDS) was calculated by the difference of SSS and SRS (18).

*Quantification of Myocardial Blood Flow (MBF).* For quantification of MBF, dynamic images were analyzed with the MunichHeart software, an established custom application that has been previously validated for quantitative PET analyses (7,19).

**TABLE 1**

General Characteristics of Reference Group Used to Define Reference Range of TID

Variable	Reference group ( $n = 62$ )
Age (y)	$49 \pm 9$
Sex	
Male	9 (15)
Female	53 (85)
Race	
Black	54 (87)
White	5 (8)
Other	3 (5)
Body mass index ( $\text{kg}/\text{m}^2$ )	$34 \pm 10$

Data in parentheses are percentages.

**TABLE 2**  
Clinical Characteristics of Entire Study Group and TID-Positive and TID-Negative Subgroups

Variable	Entire study group (n = 203)	TID negative (n = 184 [91%])	TID positive (n = 19 [9%])	P
Age (y)	60 ± 12	59 ± 12	64 ± 11	Not significant
Sex				
Men	90 (44)	79 (43)	11 (58)	Not significant
Women	113 (56)	105 (57)	8 (42)	Not significant
Race				
Black	126 (62)	117 (63)	9 (47)	Not significant
White	68 (34)	60 (33)	8 (42)	Not significant
Other	9 (4)	7 (4)	2 (11)	Not significant
Body mass index (kg/m <sup>2</sup> )	31.9 ± 8.9	32.3 ± 9.1	28.4 ± 6.7	Not significant
History of . . .				
Smoking	71 (35)	66 (36)	5 (26)	Not significant
Hypertension	134 (66)	118 (64)	16 (84)	Not significant
Hyperlipidemia	100 (49)	89 (48)	11 (58)	Not significant
Diabetes mellitus	75 (37)	68 (37)	7 (37)	Not significant
Cardiac history				
None	99 (49)	92 (50)	7 (37)	Not significant
CAD	74 (36)	62 (34)	12 (63)	<0.03
Prior MI	29 (14)	24 (13)	5 (26)	Not significant
Prior percutaneous coronary interventions or coronary artery bypass grafts	41 (20)	33 (18)	8 (42)	<0.03
Heart failure	7 (3)	7 (4)	—	Not significant
Other	44 (22)	42 (23)	2 (11)	Not significant
Obstructive CAD				
CTA	9/51 (18)	5/45 (11)	4/6 (67)	<0.006
Catheterization	28/35 (79)	23/30 (76)	5/5 (100)	Not significant
CTA or catheterization	33/81 (41)	26/72 (36)	7/9 (78)	<0.05
Medication at PET				
β-blocker	40 (20)	36 (20)	4 (21)	Not significant
Angiotensin-converting enzyme inhibitor or sartin	44 (22)	42 (23)	2 (11)	Not significant
Statin	43 (21)	39 (21)	4 (21)	Not significant

Data in parentheses are percentages.  
NS = not significant.

To determine 3-dimensional tracer distribution in the LV myocardium, volumetric sampling was accomplished, and a static polar map of 460 segments was created. Subsequently, segments were reapplied to dynamic imaging series, and time–activity curves were created. A time–activity curve of the arterial blood was calculated by a small cuboidal region of interest in the center of the LV cavity defined in short-axis planes. For the calculation of MBF, a simplified retention approach was used. Briefly, myocardial activity concentration at the time between 4 and 8 min after scan initiation was normalized to the area under the prior acquired arterial input function of the first 120 s, and the so-achieved retention index was then corrected for partial volume, spillover, and nonlinear extraction of the tracer (20–22). A study validating this approach for the PET system used at Johns Hopkins Institution was published recently by our group (7). The resting MBF is known to be influenced by the cardiac work, which can be evaluated by the rate–pressure product (23). Thus, MBF was normalized as previously described (24). The rate–pressure product was calculated by the product of heart rate and systolic blood pressure during the acquisition. Myocardial flow reserve (MFR) was then calculated as the ratio of hyperemic and resting MBF.

### Assessment of Outcome

To assess overall mortality, review of the social security death index was performed. Because of difficulties in distinguishing cardiac from noncardiac death from this index, only overall mortality was used for analysis.

### Statistical Analysis

All obtained results are shown as mean ± SD, and obtained *P* values smaller than 0.05 were considered to indicate statistical significance. The 2-tailed unpaired Student *t* test was used to compare continuous variables and the  $\chi^2$  test to compare nominal variables. To investigate the correlation between continuous variables, the Pearson coefficient with Fisher *r*-to-*z* transformation for significance was applied.

Shown survival curves were drawn according to Kaplan–Meier, and a log-rank analysis was performed to calculate *P* values. Age-adjusted multivariate Cox proportional hazards regression was performed to identify independent variables for the occurrence of defined events and to obtain exponentiation of the B coefficients (Exp[b]) and 95% confidence intervals (CIs).

For statistical analyses, MedCalc (version 11.6.1.0; MedCalc Software) for Windows (Microsoft) was used.

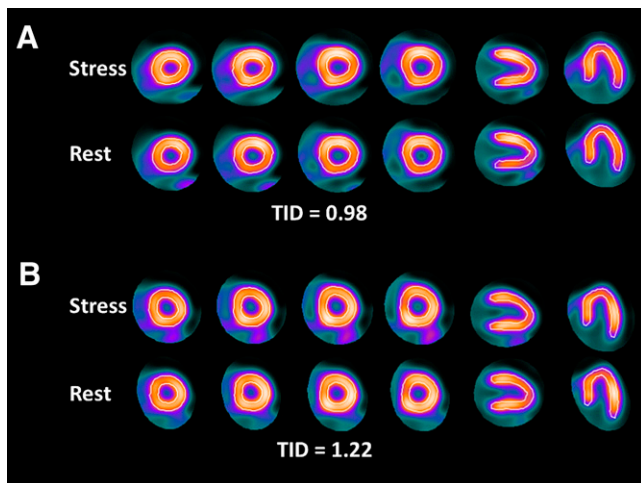


**FIGURE 1.** Assessment of TID ratio by automated contouring of left ventricle using dedicated CardIQ Physio software (GE Healthcare). Representative ungated short-axis and long-axis images at stress and at rest of patient with normal TID (A) and patient with elevated TID (B).

## RESULTS

### Establishment of Normal Range for TID

In the reference group of subjects without CAD, the TID ratio was  $0.98 \pm 0.06$ , ranging from 0.85 to 1.11. Using the mean and SD, we set a threshold for abnormally elevated TID at greater than 1.13 ( $0.98 + 2.5$  SDs) for further analysis (Fig. 2).

### Clinical Characteristics of TID-Positive Patients

In the study group with suspected or proven CAD, TID-negative ( $n = 184$ ; 91%) and TID-positive ( $n = 19$ ; 9%) subgroups were defined and compared with respect to different clinical variables (Table 2). There were no significant differences regarding age, sex, race, body mass index, history of smoking, hypertension, hyperlipidemia, or diabetes mellitus. No significant differences were found regarding

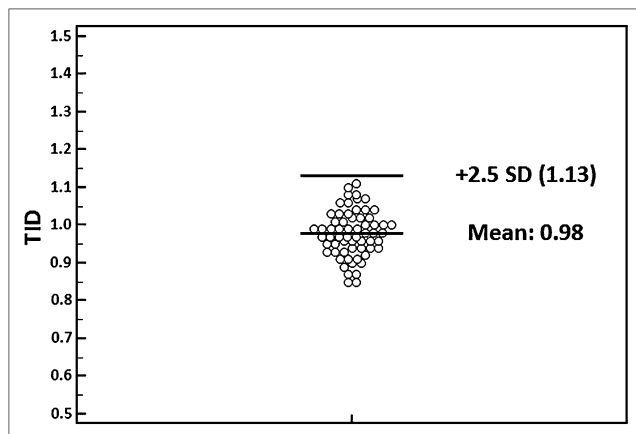


**FIGURE 2.** Dot plot representing TID values of reference group without CAD. Threshold for abnormal TID was set at greater than 1.13 ( $0.98 + 2.5$  SDs).

$\beta$ -blocker, angiotensin-converting enzyme inhibitor, angiotensin receptor blocker, or statin treatment at the time of PET acquisition. Comparing the cardiac history of both groups, we found no significant difference for prior MI, heart failure, or other cardiac diseases. Also, the rate of a negative cardiac history was similar in both subgroups. However, the rate of positive CAD history (62/184 [34%] TID-negative group vs. 12/19 [63%] TID-positive group,  $P < 0.03$ ) and the rate of prior percutaneous coronary interventions or coronary artery bypass grafts (33/184 [18%] TID-negative group vs. 8/19 [42%] TID-positive group,  $P < 0.03$ ) were significantly higher in the TID-positive subgroup. Also, obstructive CAD as assessed by CTA alone (5/45 [11%] TID-negative vs. 4/6 [67%] TID-positive group,  $P < 0.006$ ) or in combination with catheterization (26/77 [36%] TID-positive group vs. 7/9 [78%] TID-negative group,  $P < 0.05$ ) was significantly more frequent in the TID-positive subgroup. A positive TID yielded a sensitivity of 21% and a specificity of 96% for obstructive CAD using CTA or catheterization as a reference. The positive predictive value was 78% and the negative predictive value 64%.

### Relationship Among TID and LV Volumes, LV Function, Perfusion Defect Scores, Global MBF, and MFR

Table 3 outlines the results regarding LV volumes, LV function, perfusion defect scores, global MBF, and MFR for the TID-positive and -negative subgroups. Regarding LV volumes obtained from gated PET images, there was a significant difference for the change of ESV ( $\Delta$ ESV[stress–rest]) and EDV ( $\Delta$ EDV[stress–rest]) between stress and rest.  $\Delta$ ESV(stress–rest) and  $\Delta$ EDV(stress–rest) were significantly higher in the TID-positive group than in the TID-negative group ( $\Delta$ ESV[stress–rest],  $1.8 \pm 7.4$  vs.  $12.3 \pm 13.0$ ,  $P < 0.0001$ ;  $\Delta$ EDV[stress–rest],  $10.8 \pm 11.5$  vs.  $23.8 \pm 14.6$ ,  $P < 0.0001$ ). Even though there was no significant difference between the TID subgroups for the EF at stress or at rest, the EF reserve ( $\Delta$ EF[stress–rest]) was significantly smaller in the TID-positive group ( $\Delta$ EF[stress–rest],  $5.0 \pm 6.4$  vs.  $1.8 \pm 7.9$ ,  $P < 0.05$ ). Assessment of perfusion defect scores revealed significantly higher values for SSS, SRS, and SDS in the TID-positive group (SSS,  $3.0 \pm 5.4$  vs.  $7.5 \pm 9.8$ ,  $P < 0.002$ ; SRS,  $1.8 \pm 3.8$  vs.  $3.8 \pm 7.6$ ,  $P < 0.05$ ; and SDS,  $1.3 \pm 2.6$  vs.  $3.7 \pm 5.3$ ,  $P < 0.001$ ). Global MBF at rest and at stress were not significantly different between TID-positive and TID-negative patients, whereas the MFR was significantly lower in the TID-positive group ( $2.1 \pm 0.8$  vs.  $1.7 \pm 0.6$ ,  $P < 0.02$ ).

There was no correlation for ESV and EDV volumes at rest and stress with TID. However, both  $\Delta$ ESV(stress – rest) and  $\Delta$ EDV(stress – rest) were significantly correlated with TID ( $\Delta$ ESV[stress – rest]:  $R^2 = 0.23$ ;  $\Delta$ EDV[stress – rest]:  $R^2 = 0.17$ ; both  $P < 0.0001$ ). Although there was no significant correlation between the TID and EF at stress or at rest, the correlation between TID and EF reserve was also found to be significant ( $R^2 = 0.0609$ ,  $P < 0.0005$ , Fig. 3).

**TABLE 3**

LV Volume, LV Function, Perfusion Defect Scores, Global MBF, and MFR in TID-Positive and TID-Negative Subgroups

Variable	TID negative (n = 184 [91%])	TID positive (n = 19 [9%])	P
ESV rest	41.4 ± 37.8	40.2 ± 43.9	Not significant
ESV stress	43.2 ± 39.5	52.5 ± 52.7	Not significant
ΔESV (stress–rest)	1.8 ± 7.4	12.3 ± 13.0	<0.0001
EDV rest	74.7 ± 43.9	73.1 ± 51.3	Not significant
EDV stress	85.5 ± 45.5	96.9 ± 57.6	Not significant
ΔEDV (stress–rest)	10.8 ± 11.5	23.8 ± 14.6	<0.0001
EF rest	48.7 ± 12.4	50.8 ± 14.0	Not significant
EF stress	53.7 ± 13.2	52.6 ± 17.1	Not significant
ΔEF (stress–rest)	5.0 ± 6.4	1.8 ± 7.9	<0.05
SSS	3.0 ± 5.4	7.5 ± 9.8	<0.002
SRS	1.8 ± 3.8	3.8 ± 7.6	<0.05
SDS	1.3 ± 2.6	3.7 ± 5.3	<0.001
MBF rest	0.9 ± 0.3	1.0 ± 0.3	Not significant
MBF stress	1.8 ± 0.7	1.6 ± 0.8	Not significant
MFR	2.1 ± 0.8	1.7 ± 0.6	<0.02

Data are mean ± SD.

Furthermore, correlation analysis between TID and MBF at rest and stress, respectively, did not reveal any correlation, whereas MFR was weakly but significantly correlated with TID ( $R^2 = 0.0449$ ,  $P < 0.003$ , Fig. 4).

### Outcome Analysis

To determine overall mortality, patients were followed for  $969 \pm 328$  d (median, 991 d; range, 59–1,460 d) by review of social security death index. In total, 34 deaths were detected, 28 in the TID-negative subgroup and 6 in the TID-positive subgroup. The mean time to event was  $505 \pm 363$  d (median, 405 d; range, 59–1,257 d). Kaplan–Meier analysis showed that the overall survival probability was significantly smaller in TID-positive patients ( $P < 0.05$ ; hazard ratio, 2.4; 95% CI, 0.7–8.1, Fig. 5A).

Next, age-adjusted multivariate Cox proportional analysis was performed. Factors considered were functional LV impairment (EF < 45%), elevated ischemic burden (SSS > 3), reduced MFR smaller than the median in the high-risk group (MFR < 1.98), and a TID higher than 1.13. The only significantly independent predictor for an event in this analysis was an EF smaller than 45% (Table 4). Furthermore, we performed overall survival probability analysis for the subgroup of patients without regional perfusion abnormal-

ities (SSS < 4) (24,25). One hundred forty-seven subjects had normal perfusion patterns. Of those, 137 (93%) were in the TID-negative subgroup and 10 (7%) in the TID-positive subgroup. Of the 10 patients with TID but without regional perfusion defects, 8 had a reduced flow reserve below the previously validated threshold of 2.11 (24), and 5 had no prior history of CAD. Also in this subanalysis, TID-positive patients' overall survival probability was significantly smaller than that of TID-negative patients ( $P < 0.03$ ; hazard ratio, 3.8; 95% CI, 0.5–31.9; Fig. 5B). Interestingly, in this subgroup analysis, Cox regression analysis showed that positive TID was an independent predictor together with an EF below 45% (Table 5).

### DISCUSSION

Our results confirm that the upper normal limit of TID in  $^{82}\text{Rb}$  PET is within the range of previously established normal values of TID in SPECT or in planar imaging (9,10,26–28). Patients with an elevated TID show a lower EF reserve. Furthermore, in patients with an abnormal TID, ESV and EDV increase to a higher degree from rest to stress, and lower MFR and increased perfusion defect scores can be observed. The results of our preliminary out-

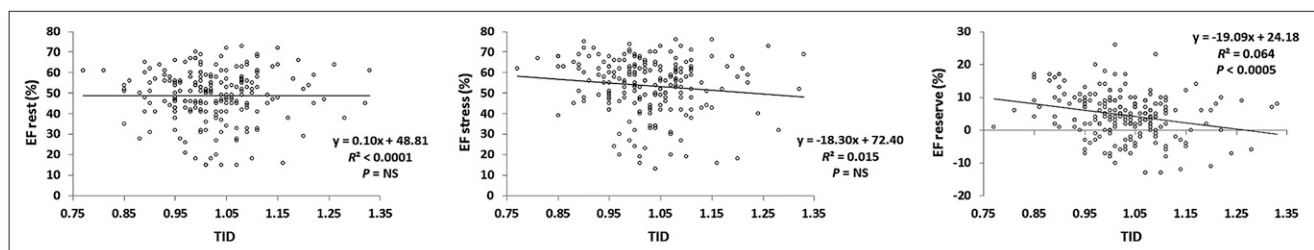


**FIGURE 3.** Correlation analysis within high-risk group shows significant correlation between EF reserve and TID. NS = not significant.

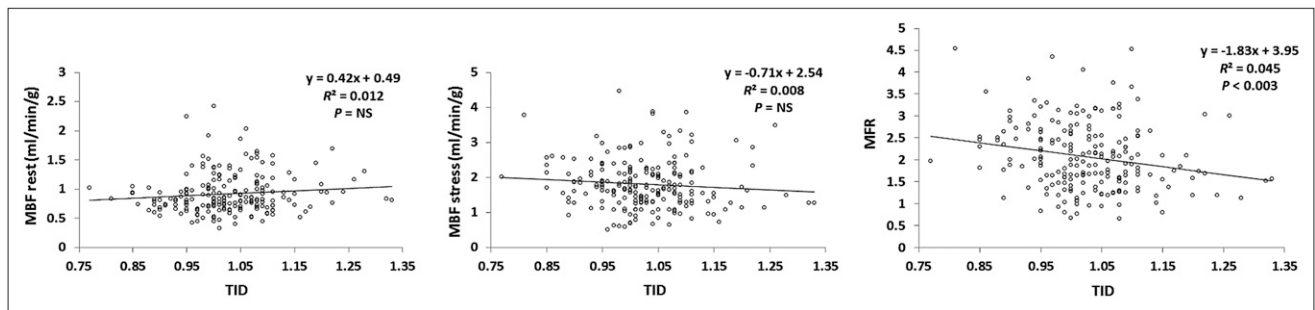


**FIGURE 4.** Correlation analysis within high-risk group shows significant correlation between MFR and TID. NS = not significant.

come analysis confirm that patients with an elevated TID are at higher risk for death. In the subgroup analysis of patients with normal regional perfusion, an abnormal TID also identified patients with higher mortality and was, moreover, an independent predictor for death together with a decreased EF.

The role of TID in the setting of  $^{82}\text{Rb}$  myocardial perfusion imaging has been only marginally investigated so far. In a prior study, Shi et al. investigated the TID ratio in  $^{82}\text{Rb}$  rest or pharmacologic stress PET and suggested an upper normal limit of 1.15. They were able to show in a small

patient group that this value yields low sensitivity but high specificity and a high positive predictive value in the diagnosis of single- and multivessel CAD (29). However, in contrast to our study, no analyses of clinical variables, LV function, MFR, or outcome were provided.

The TID ratio was described for the first time by Stolzenberg et al. in a case of planar thallium scintigraphy and has been investigated in a large number of studies including SPECT since then (30–33). Although thallium stress images are usually obtained shortly after tracer injection, stress images with  $^{99\text{m}}\text{Tc}$ -labeled tracers are ac-

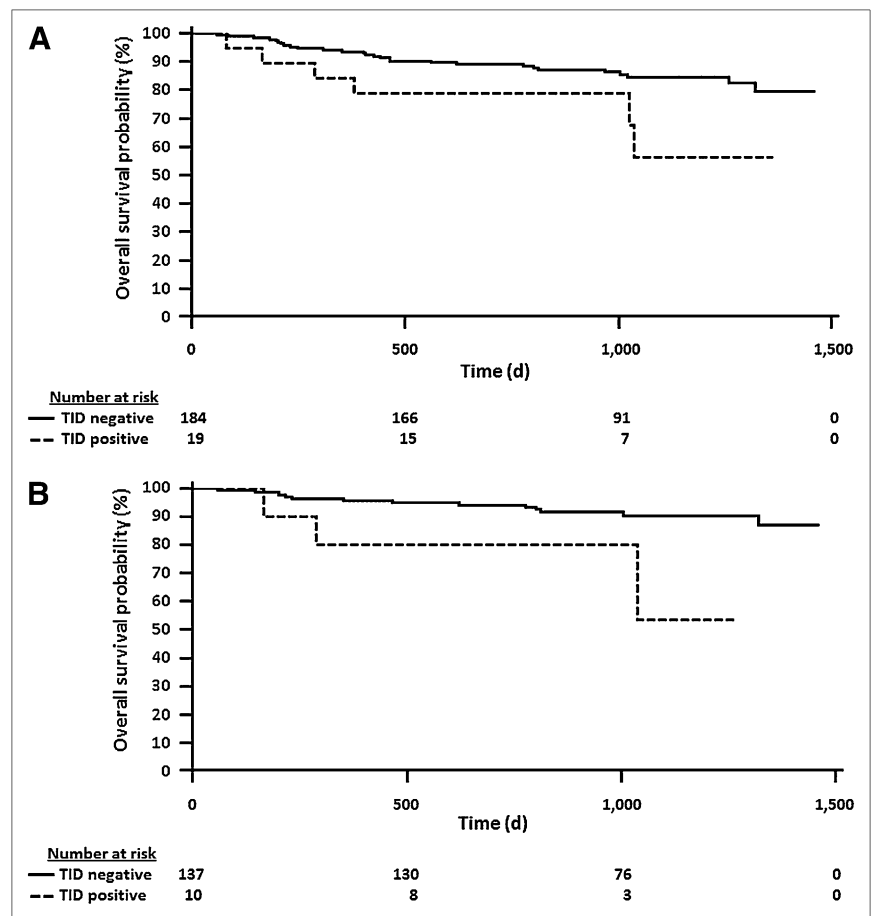


**FIGURE 5.** (A) Kaplan-Meier curve to compare overall survival probability in TID-positive and TID-negative patients ( $n = 203$ ). Overall survival probability was significantly smaller in TID-positive group ( $P < 0.05$ ). (B) Kaplan-Meier curve to compare overall survival probability in TID-positive and TID-negative subgroups without regional perfusion abnormalities defined by SSS below 4 ( $n = 147$ ). In normal-perfusion patients, overall survival probability was still significantly smaller in TID-positive group ( $P < 0.03$ ).

**TABLE 4**  
Relationship Among TID, EF, SSS, MFR, and Overall Survival Outcome Results

Variable	Exp(b)	95% CI	P
EF < 45%	3.76	1.76–8.06	<0.001
SSS > 3	1.79	0.80–3.99	0.16
TID ratio > 1.13	1.29	0.50–3.30	0.60
MFR < 1.98	1.17	0.54–2.54	0.69

Multivariate Cox regression analysis. Age-adjusted results.

quired 15–60 min after stress, depending on the protocol used. Accordingly, there are differences in the acquisition mode, and obtained results might therefore vary. In contrast to the conventional acquisition of perfusion images with  $^{99m}\text{Tc}$ -labeled perfusion agents, stress images using  $^{82}\text{Rb}$ -chloride are acquired at the peak of pharmacologic stress and at the time of tracer injection. Thus, patients have an elevated heart rate during acquisition, and the diastolic contribution to the ungated images may be reduced, leading to a reduced LV cavity size. This consideration might also explain the fact that our mean TID value in the low-risk group is slightly below 1 (0.98).

In previous publications, TID was identified as a significant predictor for adverse outcome in SPECT as well as in planar scintigraphy (10,11,33–35). However, to the best of our knowledge there are no data available so far on prognostic implications of TID in  $^{82}\text{Rb}$  PET. Our data are preliminary in this regard, because of a low number of events and relatively small sample size. But the results suggest that a positive TID is associated with a reduced overall survival probability. In a subgroup of patients with no regional perfusion defects, TID was still associated with increased risk of death. This finding is in concordance with a study by Abidov et al., who were able to demonstrate that in patients with otherwise normal myocardial perfusion SPECT, TID is a predictor of cardiac events (11). One possible explanation for a positive TID in those subjects might be triple-vessel disease. However, TID may also be a result of other cardiovascular conditions, such as cardiomyopathy, microvascular disease leading to subendocardial ischemia, or an

**TABLE 5**  
Relationship Among TID, EF, MFR, and Overall Survival Outcome Results in Subgroup Without Regional Perfusion Abnormalities

Variable	Exp(b)	95% CI	P
EF < 45%	6.16	2.07–18.32	<0.002
TID ratio > 1.13	6.22	1.60–24.25	<0.009
MFR < 1.98	1.04	0.39–2.77	Not significant

Multivariate Cox regression analysis of subgroup without perfusion abnormalities (SSS < 4). Age-adjusted results.

altered systemic hemodynamic response to vasodilator stress. Because of the small sample size and the lack of angiographic information, it is difficult to identify the underlying reason for TID in subjects without regional perfusion abnormalities in our study. Of note, 8 of 10 (80%) patients in the subset had a decreased MFR. But MFR is a complex parameter that may be associated with macroscopic triple-vessel disease but is determined by multiple factors other than potential balanced ischemia. Also, the EF reserve was decreased in patients with an elevated TID, which is most likely associated with impaired LV systolic function. Further studies with the explicit aim of clarifying the underlying cause of TID are necessary. Given the fact that TID requires no additional imaging or other data acquisition and is usually automatically calculated by the respective software, TID should always be taken into consideration when interpreting myocardial perfusion studies.

Our study has some limitations: first, it was performed retrospectively in a group that consisted of a limited number of patients who were followed up for a relatively short time. Second, our preliminary outcome analysis was restricted to the overall mortality as determined by review of the social security death index. Thus, explicit cause of death could not be assessed properly. Third, TID might be present because of triple-vessel disease. However, in the absence of angiographic or CTA results for all patients, conclusions that TID in patients with otherwise normal perfusion scans is associated with balanced ischemia should be made with extreme caution, and further studies elucidating this question need to be conducted. Fourth, because the underlying cause of TID is still not completely elucidated, there is no gold standard for the assessment of TID. As mentioned, TID has been described in various settings of SPECT and PET myocardial perfusion imaging. Thus, the suggested value of TID in this publication might only be suitable in comparable settings using comparable stressing agents and analysis software. And finally, we did not compare the occurrence of cardiac events in multiple study subgroups because follow-up could not be obtained for a sufficient time to capture a larger number of adverse events. The growing clinical use of  $^{82}\text{Rb}$  PET will allow for studies with larger sample sizes and more detailed outcome analyses in the future, to confirm our results. Our study should be seen as a stimulus for additional evaluation of TID as a prognostic marker in cardiac PET.

## CONCLUSION

Our results suggest that TID is a meaningful parameter in the setting of  $^{82}\text{Rb}$  PET myocardial perfusion imaging. The normal value of TID is less than 1.13, which is in the range of previously established values for SPECT. Similar to SPECT, a positive TID ratio is associated with more severe ischemic compromise, LV dysfunction, and reduced global flow reserve. Furthermore, our preliminary outcome analysis suggests that TID-positive subjects have a lower overall survival probability.

## DISCLOSURE STATEMENT

The costs of publication of this article were defrayed in part by the payment of page charges. Therefore, and solely to indicate this fact, this article is hereby marked "advertisement" in accordance with 18 USC section 1734.

## ACKNOWLEDGMENTS

A portion of this study was funded by research grants from GE Healthcare, Bracco Diagnostics, and Lantheus Medical Imaging. No other potential conflict of interest relevant to this article was reported.

## REFERENCES

- Bateman TM. Cardiac positron emission tomography and the role of adenosine pharmacologic stress. *Am J Cardiol.* 2004;94:19D–24D; discussion 24D–25D.
- Bengel FM, Higuchi T, Javadi MS, Lautamaki R. Cardiac positron emission tomography. *J Am Coll Cardiol.* 2009;54:1–15.
- Cecchin D, Zucchetto P, Faggin P, Bolla E, Bui F. <sup>99m</sup>Tc generator shortage: free, web-based software. *J Nucl Med.* 2010;51:14N–15N.
- Bateman TM, Heller GV, McGhie AI, et al. Diagnostic accuracy of rest/stress ECG-gated Rb-82 myocardial perfusion PET: comparison with ECG-gated Tc-99m sestamibi SPECT. *J Nucl Cardiol.* 2006;13:24–33.
- Lertsburapa K, Ahlberg AW, Bateman TM, et al. Independent and incremental prognostic value of left ventricular ejection fraction determined by stress gated rubidium 82 PET imaging in patients with known or suspected coronary artery disease. *J Nucl Cardiol.* 2008;15:745–753.
- Senthambichelvan S, Bravo PE, Esaias C, et al. Human biodistribution and radiation dosimetry of <sup>82</sup>Rb. *J Nucl Med.* 2010;51:1592–1599.
- Lautamäki R, George RT, Kitagawa K, et al. Rubidium-82 PET-CT for quantitative assessment of myocardial blood flow: validation in a canine model of coronary artery stenosis. *Eur J Nucl Med Mol Imaging.* 2009;36:576–586.
- Abidov A, Bax JJ, Hayes SW, et al. Integration of automatically measured transient ischemic dilation ratio into interpretation of adenosine stress myocardial perfusion SPECT for detection of severe and extensive CAD. *J Nucl Med.* 2004;45:1999–2007.
- Weiss AT, Berman DS, Lew AS, et al. Transient ischemic dilation of the left ventricle on stress thallium-201 scintigraphy: a marker of severe and extensive coronary artery disease. *J Am Coll Cardiol.* 1987;9:752–759.
- McLaughlin MG, Danias PG. Transient ischemic dilation: a powerful diagnostic and prognostic finding of stress myocardial perfusion imaging. *J Nucl Cardiol.* 2002;9:663–667.
- Abidov A, Bax JJ, Hayes SW, et al. Transient ischemic dilation ratio of the left ventricle is a significant predictor of future cardiac events in patients with otherwise normal myocardial perfusion SPECT. *J Am Coll Cardiol.* 2003;42:1818–1825.
- Diamond GA, Forrester JS. Analysis of probability as an aid in the clinical diagnosis of coronary-artery disease. *N Engl J Med.* 1979;300:1350–1358.
- Bravo PE, Chien D, Javadi M, Merrill J, Bengel FM. Reference ranges for LVEF and LV volumes from electrocardiographically gated <sup>82</sup>Rb cardiac PET/CT using commercially available software. *J Nucl Med.* 2010;51:898–905.
- Lautamäki R, Brown TL, Merrill J, Bengel FM. CT-based attenuation correction in <sup>82</sup>Rb-myocardial perfusion PET-CT: incidence of misalignment and effect on regional tracer distribution. *Eur J Nucl Med Mol Imaging.* 2008;35:305–310.
- Brown TL, Merrill J, Volokh L, Bengel FM. Determinants of the response of left ventricular ejection fraction to vasodilator stress in electrocardiographically gated <sup>82</sup>rubidium myocardial perfusion PET. *Eur J Nucl Med Mol Imaging.* 2008;35:336–342.
- Chander A, Brenner M, Lautamaki R, et al. Comparison of measures of left ventricular function from electrocardiographically gated <sup>82</sup>Rb PET with contrast-enhanced CT ventriculography: a hybrid PET/CT analysis. *J Nucl Med.* 2008;49:1643–1650.
- Cerqueira MD, Weissman NJ, Dilsizian V, et al. Standardized myocardial segmentation and nomenclature for tomographic imaging of the heart: a statement for healthcare professionals from the Cardiac Imaging Committee of the Council on Clinical Cardiology of the American Heart Association. *Circulation.* 2002;105:539–542.
- Hansen CL, Goldstein RA, Akinboboye OO, et al. Myocardial perfusion and function: single photon emission computed tomography. *J Nucl Cardiol.* 2007;14:e39–e60.
- Nekolla SG, Miethaner C, Nguyen N, Ziegler SI, Schwaiger M. Reproducibility of polar map generation and assessment of defect severity and extent assessment in myocardial perfusion imaging using positron emission tomography. *Eur J Nucl Med.* 1998;25:1313–1321.
- Yoshida K, Mullani N, Gould KL. Coronary flow and flow reserve by PET simplified for clinical applications using rubidium-82 or nitrogen-13-ammonia. *J Nucl Med.* 1996;37:1701–1712.
- Mullani NA, Goldstein RA, Gould KL, et al. Myocardial perfusion with rubidium-82. I. Measurement of extraction fraction and flow with external detectors. *J Nucl Med.* 1983;24:898–906.
- Mullani NA, Gould KL. First-pass measurements of regional blood flow with external detectors. *J Nucl Med.* 1983;24:577–581.
- Czernin J, Muller P, Chan S, et al. Influence of age and hemodynamics on myocardial blood flow and flow reserve. *Circulation.* 1993;88:62–69.
- Fukushima K, Javadi MS, Higuchi T, et al. Prediction of short-term cardiovascular events using quantification of global myocardial flow reserve in patients referred for clinical <sup>82</sup>Rb PET perfusion imaging. *J Nucl Med.* 2011;52:726–732.
- Ziadi MC, Dekemp RA, Williams KA, et al. Impaired myocardial flow reserve on rubidium-82 positron emission tomography imaging predicts adverse outcomes in patients assessed for myocardial ischemia. *J Am Coll Cardiol.* 2011;58:740–748.
- Kritzman J, Ficaro E, Corbett J. Post-stress LV dilation: the effect of imaging protocol, gender and attenuation correction [abstract]. *J Nucl Med.* 2001;42:50P.
- Takeishi Y, Tono-oka I, Ikeda K, et al. Dilatation of the left ventricular cavity on dipyridamole thallium-201 imaging: a new marker of triple-vessel disease. *Am Heart J.* 1991;121:466–475.
- Daou D, Delahaye N, Vilain D, et al. Identification of extensive coronary artery disease: incremental value of exercise TI-201 SPECT to clinical and stress test variables. *J Nucl Cardiol.* 2002;9:161–168.
- Shi H, Santana CA, Rivero A, et al. Normal values and prospective validation of transient ischaemic dilation index in <sup>82</sup>Rb PET myocardial perfusion imaging. *Nucl Med Commun.* 2007;28:859–863.
- Stolzenberg J. Dilatation of left ventricular cavity on stress thallium scan as an indicator of ischemic disease. *Clin Nucl Med.* 1980;5:289–291.
- Iskandrian AS, Heo J, Nguyen T, Lyons E, Paugh E. Left ventricular dilatation and pulmonary thallium uptake after single-photon emission computer tomography using thallium-201 during adenosine-induced coronary hyperemia. *Am J Cardiol.* 1990;66:807–811.
- Mazzanti M, Germano G, Kiat H, et al. Identification of severe and extensive coronary artery disease by automatic measurement of transient ischemic dilation of the left ventricle in dual-isotope myocardial perfusion SPECT. *J Am Coll Cardiol.* 1996;27:1612–1620.
- McClellan JR, Travin MI, Herman SD, et al. Prognostic importance of scintigraphic left ventricular cavity dilation during intravenous dipyridamole technetium-99m sestamibi myocardial tomographic imaging in predicting coronary events. *Am J Cardiol.* 1997;79:600–605.
- Bestetti A, Bigi R, Terranova P, Lombardi F, Fiorentini C. Prognostic implications of stress-induced transient ischemic dilation of the left ventricle in patients with systolic dysfunction and fixed perfusion defects. *Int J Cardiol.* 2010;140:323–327.
- uz Zaman M, Fatima N, Samad A, et al. Predictive and prognostic values of transient ischemic dilatation of left ventricular cavity for coronary artery disease and impact of various managements on clinical outcome using technetium-99m sestamibi gated myocardial perfusion imaging. *Ann Nucl Med.* 2011;25:566–570.



The Journal of  
NUCLEAR MEDICINE

## Transient Ischemic Dilation Ratio in $^{82}\text{Rb}$ PET Myocardial Perfusion Imaging: Normal Values and Significance as a Diagnostic and Prognostic Marker

Christoph Rischpler, Takahiro Higuchi, Kenji Fukushima, Mehrbod S. Javadi, Jennifer Merrill, Stephan G. Nekolla, Paco E. Bravo and Frank M. Bengel

*J Nucl Med.* 2012;53:723-730.  
Published online: April 9, 2012.  
Doi: 10.2967/jnumed.111.097600

---

This article and updated information are available at:  
<http://jnm.snmjournals.org/content/53/5/723>

---

Information about reproducing figures, tables, or other portions of this article can be found online at:  
<http://jnm.snmjournals.org/site/misc/permission.xhtml>

Information about subscriptions to JNM can be found at:  
<http://jnm.snmjournals.org/site/subscriptions/online.xhtml>

*The Journal of Nuclear Medicine* is published monthly.  
SNMMI | Society of Nuclear Medicine and Molecular Imaging  
1850 Samuel Morse Drive, Reston, VA 20190.  
(Print ISSN: 0161-5505, Online ISSN: 2159-662X)

© Copyright 2012 SNMMI; all rights reserved.